*Plasma Chemistry and Plasma Processing, Vol. 9, No. 4, 1989*

# Production of XeO* in a CW Microwave Discharge

M. L. Passow[1] and M. L. Brake[1]

*Received November 3, 1988; revised February 16, 1989*

*A low-power CW microwave discharge at 2.45 GHz was used to produce XeO* excimer molecules. It was found that a total gas pressure between 5 and 20 Torr, absorbed power of about 20–100 W, and an oxygen-to-xenon ratio of 1 : 100 maximized the XeO($^1S$–$^1D$) green emission at 5200 to 5600 Å. The XeO* emission appeared in the cooler parts of the discharge near the containment tube walls and in the electric field nodes of the $TM_{012}$ resonant mode.*

**KEY WORDS:** Microwave discharge; XeO; emission spectroscopy.

## 1. INTRODUCTION

The metastable states of atomic oxygen bound to ground state rare gas atoms have long been investigated.[1–14] Of prime interest is the possible use of atomic oxygen in high-energy-storage lasers. Heterogeneous excimers of oxygen have repulsive, or nearly repulsive, ground states which in principle are ideal for lower laser levels. In the case of the XeO laser, oscillation occurs between the $^1S_0$–$^1D_2$ states, the auroral line of atomic oxygen at 5571 Å, and the $^1S_0$–$^3P_1$ states, the transauroral line at 2972 Å (see Fig. 1 for a level diagram of atomic oxygen). In the presence of rare gases, a rare-gas oxide excimer is formed and the emission is considerably broadened as well as shifted.[2,3,5,6] The fact that the $^1D$ state can be deactivated rather quickly and that the ground state of XeO is repulsive, along with other properties of this system, make it an attractive candidate for a high-energy-storage laser.

The most common methods of producing the rare-gas oxide include radiofrequency discharges[1,2] at 4 MHz, positive column discharges,[3] $N_2O$ photolysis,[4,12,13] Tesla-excited discharges,[5] electron-beam discharges,[6–11] and photoexcitation.[14] In many of these studies total pressures of greater than an atmosphere were required to effectively produce the XeO* because the dissociation of $O_2$ and excitation of O($^1S$) required

[1] Department of Nuclear Engineering, University of Michigan, Ann Arbor, Michigan 48109.



0272-4324/89/1200-0497$06.00/0 

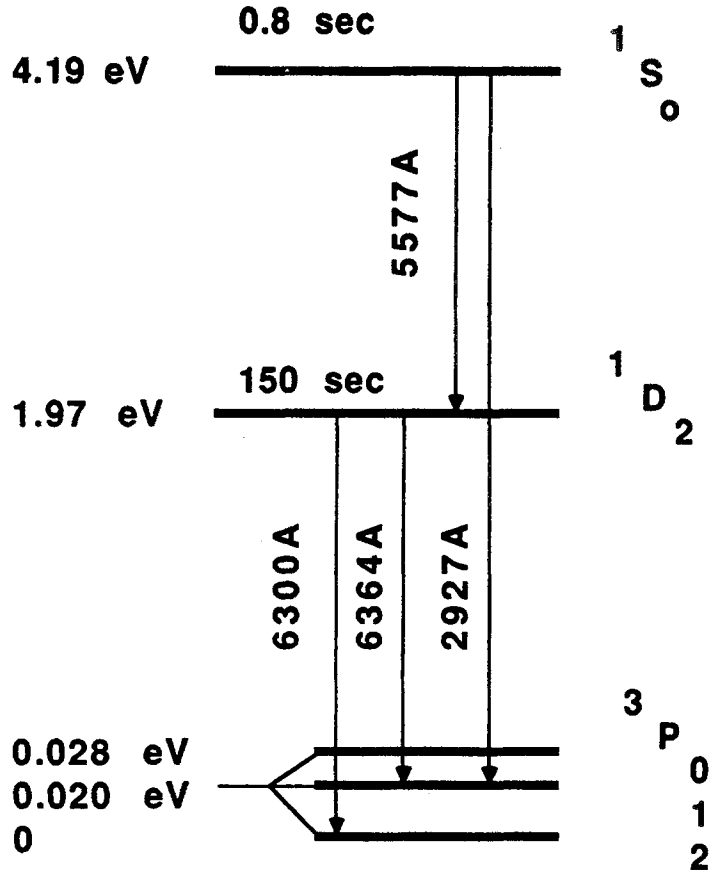


Fig. 1. Energy levels of the ground configuration of atomic oxygen. Lifetimes of the metastable terms and approximate wavelengths of the lowest-order forbidden transitions are indicated.[5]

the presence of $Xe_2^*$ molecules which are only formed at high pressures. For example, in most of the electron beam-excited discharges, the optimum concentrations were found to be a fraction of a percent of $O_2$ (up to 5 Torr) and many atmospheres of xenon (up to 16 atm). In the radiofrequency-excited discharges, the most favorable oxygen concentration was found to be around 0.01-0.05%[1,2] for total pressures of about 100 Torr to an atmosphere, and in positive column studies[3] total pressure of 3-5 Torr with about 0.5% oxygen were used.

The objective of this study was to investigate the production of the XeO* excimer using microwaves in an Asmussen resonant cavity which has been shown previously to produce high levels of oxygen dissociation at

subatmospheric pressures.[15] Steady-state excimer production as a function of power, pressure, and rare-gas-to-oxygen ratio was obtained and optimum ranges of these parameters will be discussed.

## 2. Experimental Apparatus

The experimental configuration of the discharge system is shown in Fig. 2. The plasma was contained within a 2.2 cm I.D. quartz discharge tube located coaxially within the resonant cavity. Research grade oxygen (>99.997%) and xenon (>99.995%) were metered into a 1-liter stainless steel cell for mixing. The pressure in the mixing cell was monitored with both a Pirani gauge and an absolute Heise mechanical gauge. The xenon and oxygen mixture pressure in the discharge tube was also monitored with an absolute mechanical gauge.

Both the gas mixing and gas discharge legs of the gas-handling system were evacuated to a base pressure of 5 mTorr with an 11 CFM roughing pump certified for oxygen service. The total pressure within both legs of the gas-handling system was maintained at 1 atm or less and flowing as well as static capabilities were provided.

The microwave source used was a Micro-Now magnetron oscillator which operated at 2.45 GHz. Variable magnetron current control provided for continuously adjustable power output capabilities of 0–500 W. The microwave source was protected from excessive reflected power by a coaxial circulator and dummy load.

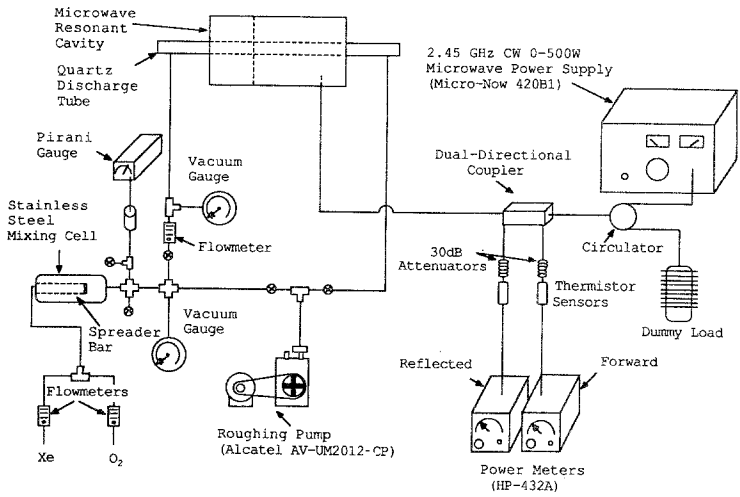


**Fig. 2.** Experimental configuration.

A coaxial dual-directional coupler was used to split off a fraction of both the forward traveling and backward traveling waves so that the incident and reflected power at the cavity could be monitored. These signals were then passed through 30-dB coaxial attenuators to the thermistor sensors of analog power meters. The output of the dual-directional coupler was connected to the input adapter on the microwave cavity coupling probe. The transmission loss of the coaxial components was measured on a Hewlett-Packard 8510 Network Analyzer. The power meter readings were calibrated to take these losses into account when determining the forward and reflected power levels. The difference between the measured incident and reflected power levels was taken to be the power absorbed by the discharge.

An Asmussen resonant cavity was formed from a brass pipe 17.8 cm I.D. A round plate, with a 5-cm-diameter hole in the center, soldered onto one end of the pipe formed the fixed short. An adjustable short at the other end of the cavity allowed for a variable resonant cavity length between 6 and 16 cm. The coupling probe insertion depth was adjustable from about 0 to 3.4 cm. By adjusting both the cavity length and the coupling probe insertion depth, different electromagnetic modes could be excited within the cavity. The two cavity modes utilized in this study were the $TM_{012}$ and $TE_{011}$ modes which have the electric field patterns shown in Figs. 3a and

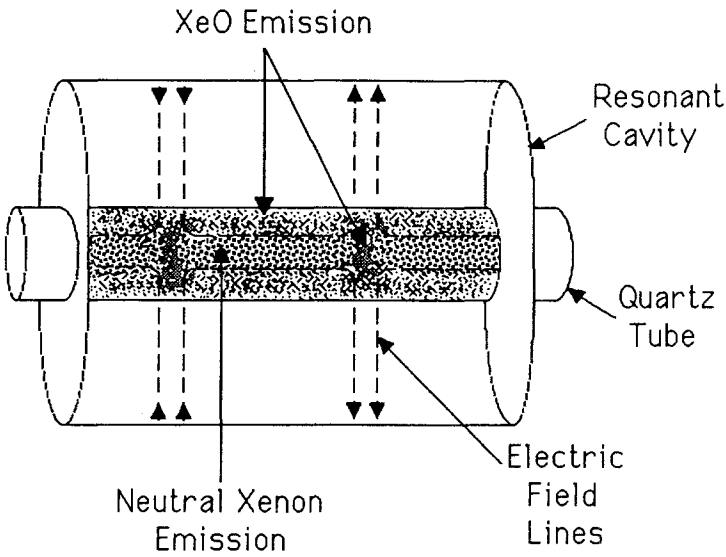


**Fig. 3a.** $TM_{012}$ electric field pattern showing the relative location of the neutral xenon and XeO* excimer emission. The excimer is produced in the nodes of the electric field and near the tube walls.

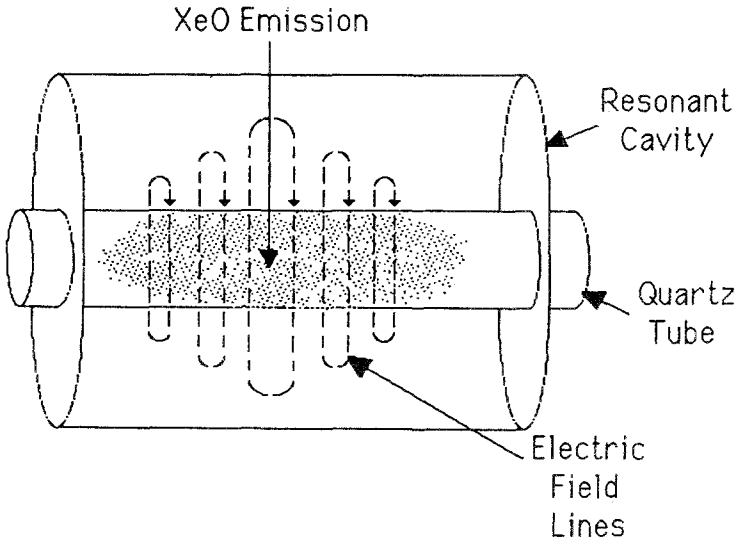


**Fig. 3b.** $TE_{011}$ electric field pattern showing the XeO* excimer production. The excimer is produced circumferentially near the tube walls.

3b, respectively. A more detailed description of the resonant cavity is given in Ref. 16.

## 3. EXPERIMENTAL RESULTS AND DISCUSSION

The discharge shape of the $TM_{012}$ plasma was such that by observing the discharge through the screened viewing port in the side of the cavity, the purple/white portion of the discharge due to the neutral xenon (verified by emission spectroscopy) was present in the high electric field regions. The green portion of the discharge due to the XeO* excimer was found near the walls of the discharge tube and in the nodes of the electric field (see Fig. 3a) In the $TE_{011}$ mode, when the conditions were such that XeO* production was possible, the discharge was almost completely green but was brightest near the tube walls (see Fig. 3b). Looking axially down the discharge tube indicated that the center of the tube was essentially void of the glowing part of the discharge and the emission was, in fact, a concentrated ring near the tube walls. Also the excimer emission was clearly more evident at the top and bottom of the discharge tube. The excimer emission seemed to be preferentially excited near the electric field regions of low magnitude and large gradient, and was not rotationally symmetric. Obviously these azimuthal nonuniformities need to be removed if the whole discharge volume is going to be used as a laser gain medium. In general,

the discharge is bright enough to be used as a spectroscopic source, particularly if apertures are used to select uniform regions of the discharge. The mechanisms of the spatial nonuniformities are still under investigation.

Emission spectroscopy was used to monitor the plasma performed over the range of 1600–8400 Å. By monitoring select Xe(I) atomic emission lines, excimer continuum levels, and excimer vibrational band emission, relative changes in species production were measured. The emitted light was collected with a short-focal-length lens placed at the end of the long discharge tube such that all of the light along the discharge tube was collected. The discharge emission was also examined perpendicular to the axis through the screened opening on the side of the resonant cavity. The light was focused onto the entrance slit of either a 0.25-m spectrograph or a 1-m spectrograph. The intensity was measured with an intensified optical multichannel analyzer.

A pure xenon discharge gave neutral xenon lines while a pure oxygen discharge produced $O_2^+$ and a few $N_2$ impurity lines [mainly $N_2(C^3\Pi\text{-}B^3\Pi)$]. No atomic oxygen emission was observed. A yellow-green continuum due to $NO_2$ formation from oxygen atoms and nitrogen impurities was observed at higher pressure mixes of $Xe + O_2$ and at higher $O_2$:Xe ratios. Depending upon discharge conditions, XeO* emission was observed for Xe:$O_2$ ratios ranging from 10,000:1 to 1:1 and pressures from 5 to 50 Torr. Emission from the transauroral transition is shown in Fig. 4a as a broad continuum centered near 3100 Å, and the auroral emission bands are shown in Figs. 4b and 4c progressing from ~5150 to ~5580 Å. The vibrational level emission is observed; however, the rotational fine structure is not resolved due to the overlapping of the rotational bands at room temperatures and above.[2] The major line emissions between 3900 and 6500 Å were due to neutral xenon.

By monitoring a portion of the green excimer emission spectrum relative to the underlying continuum while collecting the light in the axial direction, the XeO* emission intensity was investigated as a function of pressure. With an absorbed power of 22 W the pressure response was monitored for each $O_2$:Xe mixture of $1:10^4$, $1:10^3$, $1:10^2$, and 1:10 (see Fig. 5). The 1:100 mix showed the highest excimer emission at about 10 Torr and decreased with increasing pressure. The two rarer mixtures, $1:10^3$ and $1:10^4$, showed a relatively slow change over the 1–40 Torr range. The excimer emission of the oxygen-rich 1:10 mixture dropped rapidly as the pressure increased and the discharge extinguished above 15 Torr.

There are two possible explanations for the pressure dependence of the XeO* emission. The $O(^1S)$ state is more quickly deactivated by O and $O_2$ with a rate of $7.5 \times 10^{-12}$ and $3.6 \times 10^{-13}$ $cm^3/sec$, respectively,[17] compared to xenon, which has a deactivation rate of around $2 \times 10^{-15}$ $cm^3/sec$.

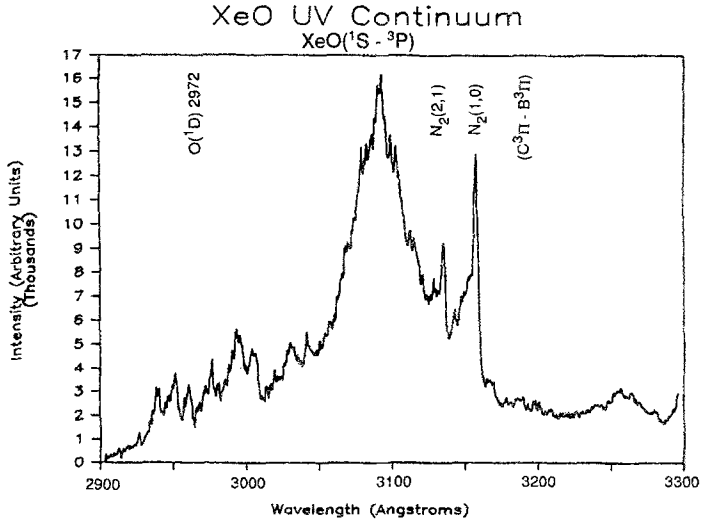


**Fig. 4a.** Spectral emission of the XeO($^1S$-$^3P$) transition in the UV. The continuum emission is shown to peak at ~3100 Å.

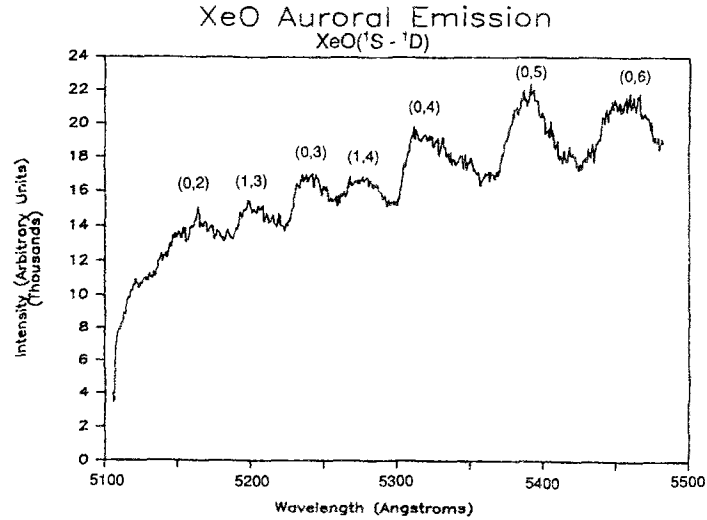


**Fig. 4b.** Spectral emission of the XeO($^1S$-$^1D$) transition in the green with the vibrational levels given for emission between 5100 and 5500 Å.

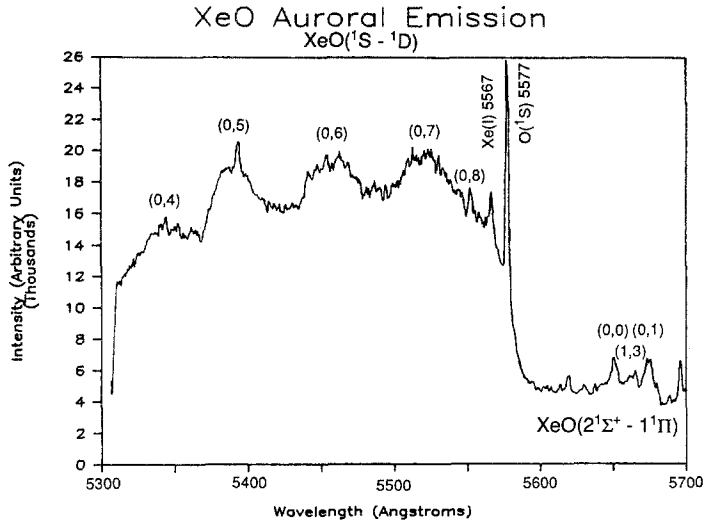


**Fig. 4c.** Spectral emission of the XeO($^1S$-$^1D$) transition in the green with the vibrational levels given for emission between 5300 and 5600 Å.

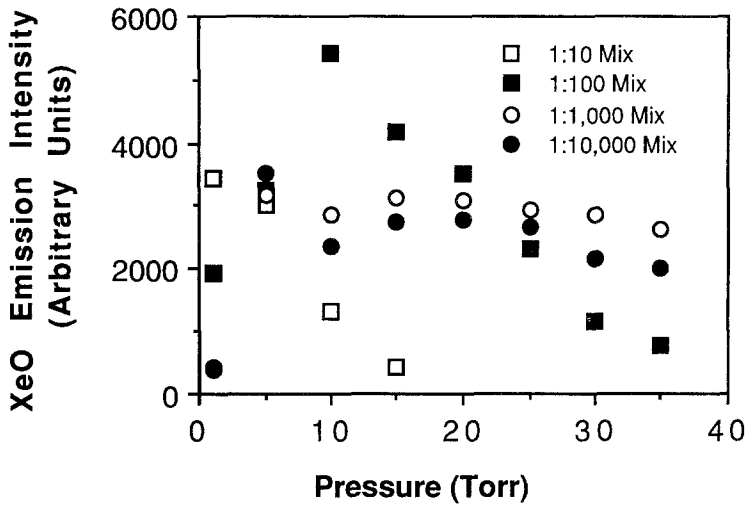


**Fig. 5.** XeO* emission intensity as a function of pressure at a constant power of 22 W for the $O_2$:Xe mixtures indicated.

Since the formation of XeO* depends directly on the $O(^1S)$ concentration through the reaction

$$O(^1S)+Xe+Xe \rightarrow XeO^*+Xe \tag{1}$$

increased deactivation would decrease XeO* emission even if the Xe concentration increased. Therefore for higher ratios of $O_2$:Xe mixtures there is more oxygen available to deactivate the $O(^1S)$ particularly as the overall pressure is increased.

Obviously, the formation of XeO* also depends upon the amount of dissociation of molecular oxygen and the degree of excitation of the resulting oxygen atoms. As discussed in Ref. 15, the degree of dissociation occurring in microwave discharges decreases at pressures above about 8 Torr mainly because of wall recombination

$$O \rightarrow \tfrac{1}{2}O_2 \tag{2}$$

and volume recombination

$$O+O+M \rightarrow O_2+M \tag{3}$$

where M can be $O_2$, O, or Xe. The main mechanism of $O(^1S)$ production is either through electron impact excitation

$$e+O \rightarrow O(^1S)+e \tag{4}$$

or energy transfer with metastable xenon atoms

$$Xe^*+O \rightarrow Xe+O(^1S) \tag{5}$$

The excitation of xenon metastables as well as excitation of xenon levels which undergo allowed transitions are also assumed to occur via electron impact excitation. This should increase with pressure and electron density but, as is seen in Fig. 6, the emission from the allowed atomic xenon transition at 4671 Å decreases dramatically with increasing pressure. It is well known that the volume of the plasma excited by a microwave resonant cavity changes with changing pressure and power.[18] Atomic oxygen emission as well as $O_2^+$ emission is typically not observed for xenon/oxygen discharges. So, under most discharge conditions with a 1:100 mix, the atomic oxygen is either quickly lost due to recombination reactions (2) and (3) or used in the production of XeO* via reaction (1). Since xenon excitation and atomic oxygen production are dependent upon electron impact processes (4) and (5), it is difficult to determine the exact excitation and relaxation mechanisms and hence the fractional energy deposition without knowing the volume of the plasma or the electron density.

For higher $O_2$:Xe ratios it was more difficult to sustain the discharge because, in general, it takes more power to sustain a discharge of a molecular gas compared to the amount needed to sustain the same amount of a rare

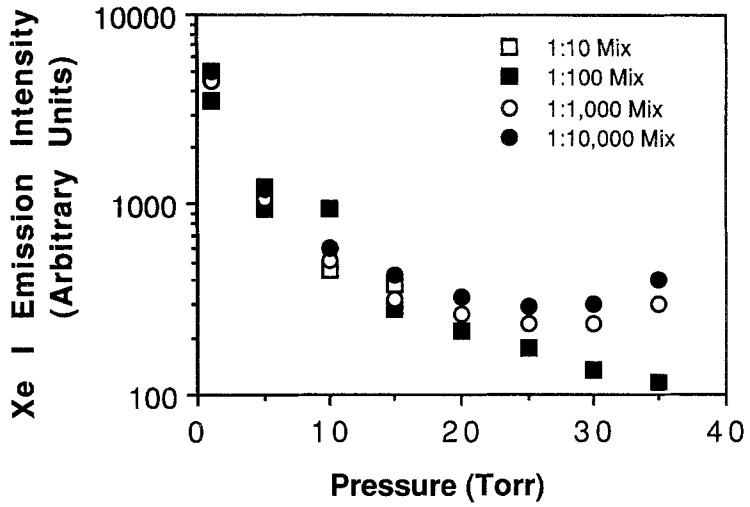


**Fig. 6.** Neutral xenon 4671 Å emission intensity as a function of pressure at a constant power of 22 W for the $O_2$:Xe mixture ratios indicated.

gas, particularly as the pressure is increased. Therefore, as the molecular oxygen concentration becomes substantial, it takes more and more power to keep the discharge going, until the incoming power can no longer maintain breakdown. This is due to the fact that molecular gases have more energy pathways such as dissociation, rotational and vibrational excitation, etc., to be included in the overall energy balance of the system. Therefore, at higher partial pressures of $O_2$, it is more difficult to maintain the discharge.

An interesting effect was observed when the discharge was taken to a high pressure (~50 Torr) and then reduced in pressure to about 10–30 Torr by letting some of the gas mixture out through the vacuum system. The XeO* emission increased to levels above that normally found at these pressures; the XeO* emission intensity remained fairly large as the flow was reduced to zero, where it then decreased to the optimum steady-state intensities, i.e., static discharge conditions. It is possible that the electric field pattern may change or some convective cooling may occur which could change the temperature-dependent rates of formation.

The ratio of the green XeO* emission to the xenon emission at 4671 Å is shown as a function of pressure in Fig. 7. Note that the XeO*-to-Xe ratio is approximately the same for all mixes and is approximately constant for pressures greater than 10 Torr.

The XeO* production for the 1 : 100 mixture of $O_2$ : Xe increased slightly for absorbed power in the 20–60 W range and then decreased slightly, as

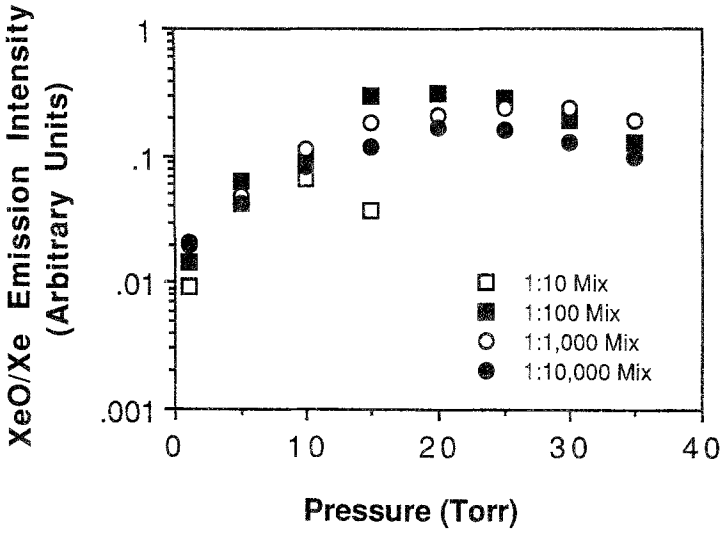


Fig. 7. Ratio of XeO* emission to neutral xenon emission as a function of pressure at a constant power of 22 W for the $O_2$:Xe mixture ratios indicated.

is seen in Fig. 8. The XeO* emission increased with increasing power for the 1:10 emission although the yellow green glow due to $NO_2$ production may have added to the XeO* signal for large powers. Power did not greatly affect the rare mixes of oxygen to xenon. Again the volume of the plasma tended to increase for higher powers to keep the power density approximately constant.[18] On the other hand, the Xe emission steadily increased with increasing power, as shown in Fig. 9, except for the case of the rarest

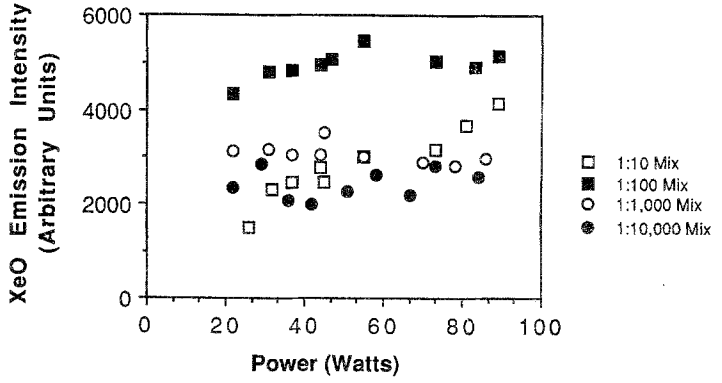


Fig. 8. XeO* emission intensity as a function of power at a constant pressure of 10 Torr for the $O_2$:Xe mixture ratios indicated.

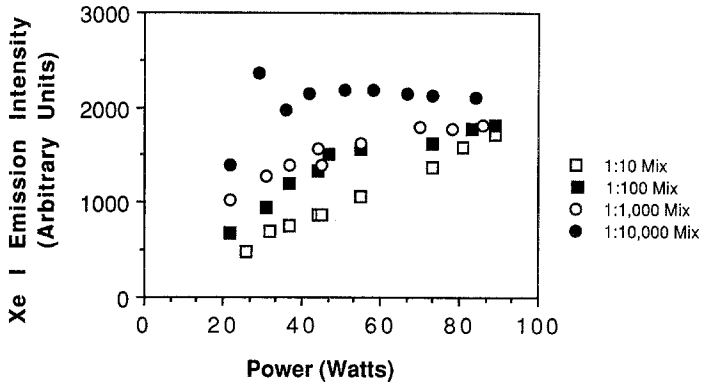


**Fig. 9.** Neutral xenon 4671 Å emission intensity as a function of power at a constant pressure of 10 Torr for the $O_2$:Xe mixture ratios indicated.

oxygen-to-xenon mixture of 1:10,000. The total pressure was kept constant at 10 Torr for this study and, therefore, as the amount of $O_2$ is increased with increasing $O_2$/Xe ratio, the amount of xenon decreases. Therefore the rarer mixtures of $O_2$:Xe would be expected to give a larger overall xenon emission signal due to the fact that these mixtures contained larger partial pressures of Xe. The overall ratio of XeO* to Xe is shown in Fig. 10 as a

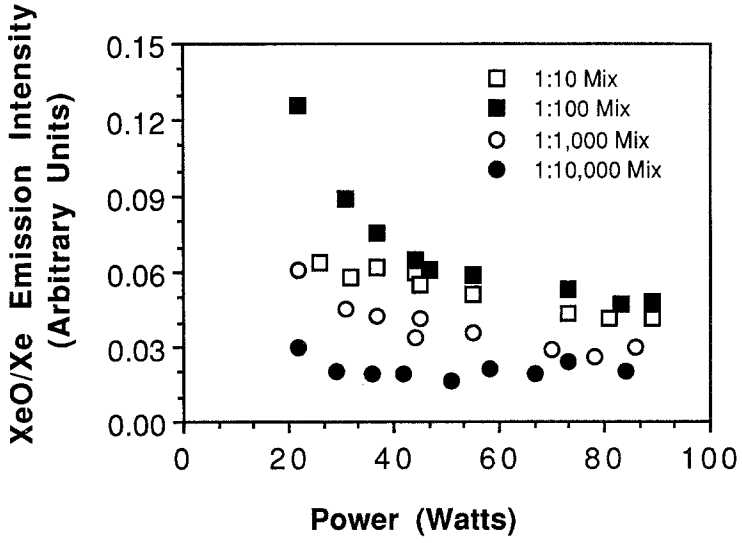


**Fig. 10.** Ratio of XeO* emission to neutral xenon emission as a function of power at a constant pressure of 10 Torr for the $O_2$:Xe mixture ratios indicated.

function of power and, as can be seen, this ratio is fairly insensitive to power, except for the 1:100 mix, where the XeO*/Xe ratio monotonically decreases with increasing power. Note that the decrease in the XeO*/Xe ratio for the 1:100 mix is due to an increase in Xe(I) emission with increasing power, seen in Fig. 9, and is *not* due to a decrease in XeO* emission, since, as seen in Fig. 8, the XeO* emission remains constant with power.

The xenon electronic temperature, found by comparing the line intensities at 4501 and 4671 Å, is given as a function of pressure in Fig. 11. As the pressure increased, the electronic temperature stayed about the same for all the gas mixtures except for the 1:100 mixture where it increased with pressure. At this mixture the amount of XeO* is large, which may indicate that when the XeO* collisionally dissociates, one of the xenon atoms may be left in an excited state rather than the ground state as follows:

$$XeO^* + Xe \rightarrow O + Xe + Xe^* \tag{6}$$

As a function of power the electronic temperature decreased slightly although this is probably within the limits of the accuracy of this technique (see Fig. 12).

The exact degree of dissociation of molecular oxygen is unknown at this time. In a similar microwave system, 100% dissociation was produced in pure oxygen discharges at 8–16 Torr with 500 W of absorbed power. In

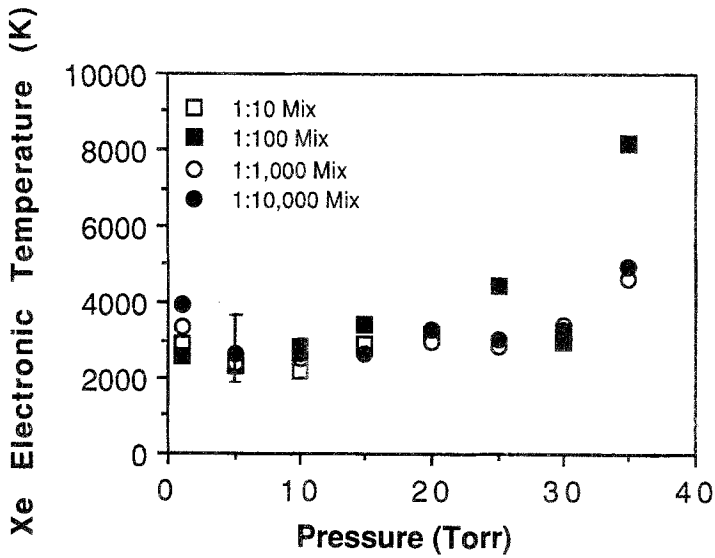


**Fig. 11.** Neutral xenon electronic temperature as a function of pressure at a constant power of 22 W for the $O_2$:Xe mixture ratios indicated. The temperatures were determined from the emission intensity ratios of the 4501 Å line and the 4671 Å line.

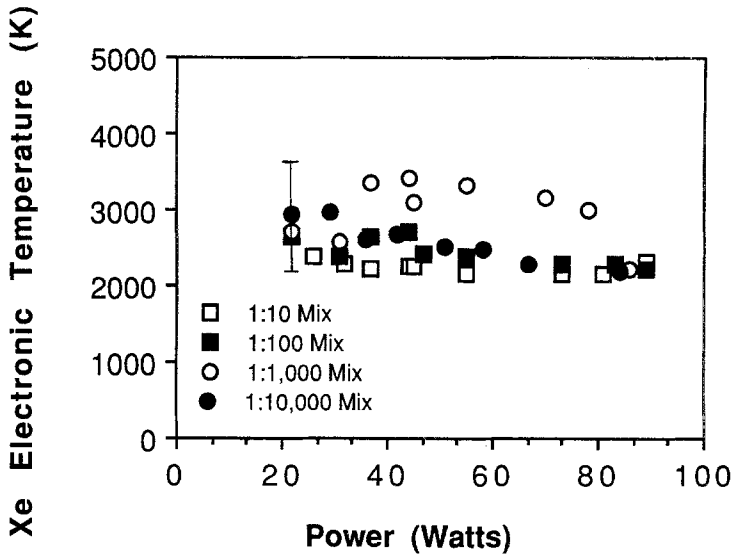


**Fig. 12.** Neutral xenon electronic temperature as a function of power at a constant pressure of 10 Torr for the $O_2$:Xe mixture ratios indicated. The temperatures were determined from the emission intensity ratios of the 4501 Å line and the 4671 Å line.

xenon/oxygen discharges of the same pressure but lower power, emission from either atomic oxygen or $O_2^+$ was rarely observed. Due to the lack of prominent emission from neutral molecular oxygen, it is difficult to even estimate the degree of dissociation. However, at 20 Torr and 293 K (very little heating was seen at 22 W), the maximum number of oxygen atoms available assuming 100% dissociation is $1.3 \times 10^{16}$ cm$^{-3}$. A threshold inversion population of about $5 \times 10^{13}$ was calculated for a photolytically pumped laser[12] assuming typical laser losses. This photolytically pumped laser[12] produced a population inversion of about $1 \times 10^{14}$ cm$^{-3}$ and measured a small signal gain of $3.5 \times 10^{-3}$ cm$^{-1}$. A microwave-pumped XeO laser could produce similar results if even a modest degree of dissociation could be achieved and if the problem of discharge spatial nonuniformity could be resolved.

## 4. CONCLUSIONS

Maximum XeO* production was observed using emission spectroscopy at an $O_2$:Xe ratio of 1:100, a total pressure of 5–20 Torr, and 20–100 W of absorbed power. The most intense XeO* emission occurred near the discharge tube walls of the $TE_{011}$ mode and near the walls and in the nodes

of the $TM_{012}$ electric field resonant mode structure. Higher-pressure discharges reduced XeO* production due to collisional deactivation of the $O(^1S)$ state as well as reduced degree of dissociation.

## ACKNOWLEDGMENTS

This project was supported by the Michigan Memorial Phoenix Project and the Office of the Vice President for Research at the University of Michigan. The authors would also like to gratefully acknowledge the technical advice of Professor Jes Asmussen.

## REFERENCES

1. C. Kenty, J. Aicher, and E. Noel, *J. Phys. Rev.* **69**, 36, 1946.
2. C. D. Cooper, G. C. Cobb, and E. L. Tolnas, *J. Mol. Spectrosc.* **7**, 223 (1961).
3. M. Yamagishi, *J. Quant. Spectrosc. Radiat. Transfer* **30**, 61, 1983.
4. J. R. Murray and C. K. Rhodes, "The possibility of a high-energy-storage visible laser on the auroral line of oxygen," University of California Lawrence Livermore Laboratory, Report UCRL-51455 (1973).
5. D. L. Cunningham and K. C. Clark, *J. Chem. Phys.* **61**, 1118 (1974).
6. H. T. Powell, J. R. Murray, and C. K. Rhodes, *Appl. Phys. Lett.* **25**, 730 (1974).
7. D. L. Huestis, R. A. Gutcheck, R. M. Hill, M. V. McCusker, and D. C. Lorents, "Studies of E-beam pumped molecular lasers," Stanford Research Institute Report SRI No. MP 75-18 (1975).
8. D. C. Lorents and D. L. Huestis, "Excimer and energy transfer lasers," *Lecture Notes in Physics*, Vol. 43, *Laser Spectroscopy*, Springer, New York (1975), p. 100.
9. J. R. Murray, H. T. Powell, and C. K. Rhodes, "The oxygen auroral transition laser system excited by collisional and photolytic energy transfer," *Lecture Notes in Physics*, Vol. 43, *Laser Spectroscopy*, Springer, New York (1975), p. 239.
10. N. G. Basov, A. N. Brunin, V. A. Danilychev, A. G. Degtyarev, V. A. Dolgikh, O. M. Kerimov, and A. N. Lobanov, *Sov. J. Quantum Electron.* **6**, 934 (1976).
11. J. R. Murray and C. K. Rhodes, *J. Appl. Phys.* **47**, 5041 (1976).
12. V. S. Zuev, L. D. Mikheev, and I. V. Pogorel'skii, *Sov. J. Quantum Electron.* **9**, 884 (1979).
13. V. S. Zuev, L. D. Mikheev, and I. V. Pogorel'skii, *Sov. J. Quantum Electron.* **10**, 853 (1980).
14. N. K. Bibinov and I. P. Vinogradov, *Sov. J. Quantum Electron.* **12**, 594 (1982).
15. M. Brake, J. Hinkle, J. Asmussen, M. Hawley, and R. Kerber, *Plasma Chem. Plasma Process.* **3**, 63 (1983).
16. J. Asmussen, R. Mallavarpu, J. Hamann, and H. Park, *Proc. IEEE* **62**, 109 (1974).
17. M. V. McCusker, "The rare gas excimers," *Topics in Applied Physics*, Vol. 30, *Excimer Lasers*, Ch. K. Rhodes, ed., Springer, N.Y. (1984), p. 47.
18. J. R. Rogers, Ph.D. thesis, Michigan State University, 1982.